Instabilities in a Magneto-optical Trap: Noise-Induced Dynamics in an Atomic System

David Wilkowski,* Jean Ringot, Daniel Hennequin, and Jean Claude Garreau

Laboratoire de Physique des Lasers, Atomes et Molécules, Unité mixte du Centre National de la Recherche Scientifique, Centre d'Etudes et de Recherches Lasers et Applications, Bâtiment P5, Université des Sciences et Technologies de Lille, F-59655 Villeneuve d'Ascq cedex, France

(Received 29 November 1999)

The instabilities observed in the atomic cloud of a magneto-optical trap are experimentally studied through the dynamics of the center of mass location and the cloud population. Two dynamical components are identified: a slow, stochastic one affects both variables, and a fast, deterministic one affects only the center of mass location. A one-dimensional stochastic model taking into account the shadow effect is developed from these observations and reproduces the experimental behavior. It is shown that instabilities are driven by noise and present stochastic resonancelike characteristics.

PACS numbers: 32.80.Pj, 05.40.Ca, 05.45.–a

The cooling of atoms in magneto-optical traps (MOT) is now extensively used to study the atom properties, or as an intermediate stage in a more complex setup, to make, e.g., lattices or Bose-Einstein condensates [1]. Surprisingly, the collective dynamics of the cold atomic cloud produced by such a system has seldom been studied, except in the case where the trapping beams are misaligned [2,3]. In that situation, ring-shaped clouds and chaos have been observed, and attributed to a vertex force. With well aligned beams and highly populated trap, cloud shape instabilities are often observed. However, to our knowledge, no systematic studies of these instabilities have been performed so far, leaving several fundamental points unexplained: Is the dynamics deterministic or stochastic? What are the critical parameters and the physical mechanisms leading to the instabilities? The main aim of this paper is to identify these mechanisms and to characterize the instabilities.

We work with a cesium-atom MOT in the usual σ_+-σ_- configuration. Each of the three arms of the trap is formed by counterpropagating beams resulting from the reflection of the three forward beams, obtained from the same laser diode. Two 4-quadrant photodiodes (4QP) forming an orthogonal dihedral (preventing stray line-of-sight effects) allow us to monitor the 3D motion of the center of mass (c.m.) of the cloud [4]. The number of atoms inside the cloud is deduced from the total signal received by the 4QPs.

Instabilities consist in a deformation of the spatial atomic distribution, leading to fluctuations of the c.m. location $\mathbf{r}$ and of the number of atoms n in the cloud. Instabilities occur only in limited ranges of the MOT parameters, e.g., MOT detunings between -1.3Γ and -0.9Γ for a trap beam intensity of 4.4 mW/cm^2 and a magnetic field gradient of 14 G cm^{-1} (Γ is the natural width of the atomic transition), corresponding to a cloud diameter of 1 mm. Instabilities also depend on other parameters, such as the cesium vapor pressure in the cell, and always appear for strong populated clouds (mean atom number larger than 10^8, corresponding to an optical thickness of 2). Note that all the above parameters affect the mean cloud population, and that instabilities can be observed for a wide variety of parameters.

The typical unstable behavior of $\mathbf{r}$ appears as an erratic signal interrupted by almost periodic oscillations with large amplitude, referred to in the following as *relaxation oscillation behavior* (Fig. 1). The spectrum of the $\mathbf{r}$ components shows a peak (Fig. 2a) centered at a frequency ν_r, which depends on the parameter values, but ranges typically between 10 and 100 Hz. It also exhibits a low frequency component below $\nu_n \approx 5$ Hz, which displaces the cloud along the first bisector of the three forward beams. The dynamics of n for the same parameters is quite different: it is erratic, and shows only frequencies below ν_n, and no peak (Fig. 2b). Analysis of the n behavior using the standard tools of nonlinear dynamics analysis (reconstruction of the attractor, Poincaré sections, 1D maps, ...) [5] have not evidenced any order in the n dynamics, and we conclude that this dynamics is stochastic. Although the behaviors of $\mathbf{r}$ and n seem drastically different, they are found to be correlated when the frequency components larger than ν_n are filtered, with a cross correlation coefficient of the order of 0.8. Figure 3 shows a phase space projection of the low frequency component of the dynamics. It illustrates the correlation between n and $\mathbf{r}$, and shows

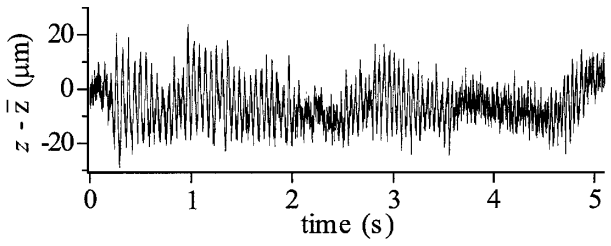

FIG. 1. Experimental record of the time evolution of a component of the c.m. location of the atomic cloud, characterized by the relaxation oscillation behavior. Experimental parameters are the following: each trap beam intensity 6.6 mW/cm^2, trap detuning -1.5Γ, and magnetic field gradient 14 G/cm. The *mean* cloud population is 1.52×10^8 atoms and the cloud size is 1 mm.

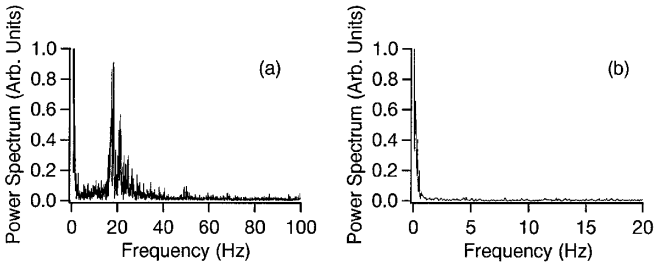

FIG. 2. Power spectra corresponding to the behavior illustrated in Fig. 1. In (a) c.m. location, and in (b) cloud population. The scales are linear.

evidence of an inhomogeneous distribution of the trajectories, with two maxima in the probability distribution. The behavior reported above is qualitatively independent of the parameters.

The relative magnitude of the observed low frequency stochastic fluctuations of the cloud population is of the order of 10^{-2}, in which the $1/\sqrt{n}$ noise contributes for a negligible amount of 10^{-4}. We could not identify the origin of the stochastic dynamics, but we checked that it was not a linear response of the system to technical noise. We paid special attention to the stability of the relative phases of the beams, and checked that their drifts are less than 0.1 rad per minute. Moreover, we voluntarily modulated the relative phase of the counterpropagating beams at different frequencies and observed a linear response of the c.m. motion only at low frequencies. The instabilities survived to fast modulation (>1 kHz) of this phase, strongly suggesting that they are not related to Sisyphus-like effects.

Two kinds of nonlinearity are known to affect the collective behavior of cold atom clouds: multiple scattering and the shadow effect [6,2]. Multiple scattering [2] arises when a photon spontaneously emitted by an atom in the cloud is absorbed by another one. However, as it is an *internal* force, it cannot directly affect the c.m. motion [7].

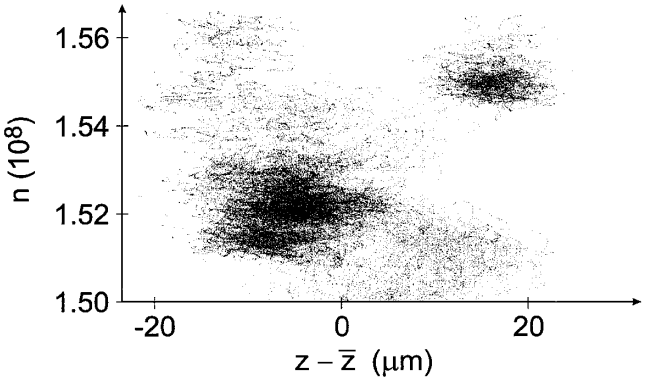

FIG. 3. Experimental dynamics of the atomic cloud instabilities represented in the phase space (n, z). The temporal behavior corresponds to that of Fig. 1, for a total duration of 10 s, encompassing several periodic sequences. The frequencies larger than 5 Hz have been filtered. There is a clear correlation between n and z and two preferred areas.

The shadow effect is due to the intensity gradients produced by the absorption of the trapping lasers by the cloud itself. It depends on the optical thickness of the cloud, and thus on its population. This effect generates a force compressing the atoms in the cloud [2]. In the reflected beam MOT configuration, it also generates an imbalance between the forward and backward trapping beams, resulting in a force that displaces the c.m. The observed correlation between the n and slow c.m. dynamics suggests that the shadow effect is the dominant nonlinearity [8]. An additional evidence of this role is given by the fact that the slow dynamical component of $\mathbf{r}$ displaces the cloud along the first bisector of the three forward beams.

We built a simple 1D model taking into account the shadow effect. Considering the dynamics of the c.m. along the z axis, we calculate the mean Doppler force per atom. We take into account the shadow effect by considering that the intensity of the backward beam is equal to the intensity of the forward beam *attenuated* by the absorption of the cloud, which depends on its population (we thus neglect the intensity gradients *inside* the cloud). The cloud population is governed by a "feed-loss" rate equation [9]. We thus find the following equations of motion:

$$\frac{d^2z}{dt^2} = \frac{1}{m} F_T \,, \tag{1a}$$

$$\frac{dn}{dt} = B(n_e - n) \,, \tag{1b}$$

where m is the mass of an atom, F_T the total force per atom, n_e the atom number in the cloud at equilibrium, and B the population relaxation, typically $B \approx 3\ \mathrm{s}^{-1}$.

The origin of z coincides with the "trap center," that is, the zero of the magnetic field. Because of the absorption of the forward beam of intensity I_+, the backward beam has an intensity $I_- = I_+ e^{-\alpha}$. I_+ and I_- are normalized with respect to the saturation intensity. The absorption coefficient α is related to the absorption cross section σ_A by [2,10]

$$\alpha = -\frac{\sigma_A}{S} n = -\frac{6\pi}{k^2} \frac{1}{1 + 4\Delta_+^2 + I_T} \frac{n}{S} \,, \tag{2}$$

where S is the section of the cloud, $I_T = I_+ + I_-$ the total intensity, and k the wave number of the beam. Δ_+ (Δ_-) is the detuning of the forward (backward) beam normalized to Γ, the natural width of the transition. They are given by

$$\Delta_\pm = \frac{1}{\Gamma} (\Gamma\Delta_0 \mp k v \mp \omega_B' z) \,, \tag{3}$$

where Δ_0 is the MOT detuning normalized to Γ, and ω_B' is the Zeeman shift in angular frequency per unit length. The force $F_\pm$ acting on an atom following the $\pm z$ direction can be written as [2,10]

$$F_\pm = 2\hbar k \Gamma \frac{I_\pm}{1 + 4\Delta_\pm^2 + I_T} \,, \tag{4}$$

and the total force is therefore $F_T = F_+ - F_-$.

We must also take into account the dependence of the stationary population n_e on the c.m. position. We do not know the exact form of this dependence but, for our purposes, it is enough to suppose that it varies smoothly over the typical amplitude of the c.m. motion, and then keep just one term from its Taylor's series. The linear term is ruled out by symmetry considerations and we write

$$n_e = n_0\left[1 - \left(\frac{z}{z_0}\right)^2\right], \tag{5}$$

where n_0 is the cloud population at the trap center and $z_0 = 6$ cm a characteristic length obtained by comparison of the simulations with the experimental signals. The very large value of z_0 confirms that n_e varies smoothly as the c.m. is displaced. The numerical results presented below do not depend critically either on the precise algebraic form of $n_e(z)$ or on the value of z_0.

Introducing the reduced variables $Z = z/z_0$ and $N = n/n_0$, we obtain finally the following equations

$$\frac{d^2Z}{dt^2} = \frac{2\hbar k\Gamma}{mz_0} I_+\left(\frac{1}{1 + 4\Delta_+^2 + I_T} - \frac{e^{-\alpha}}{1 + 4\Delta_-^2 + I_T}\right), \tag{6a}$$

$$\frac{dN}{dt} = B(1 - Z^2 - N)\,. \tag{6b}$$

The stationary solution for the c.m. (population) is Z_s ($N_s = 1 - Z_s^2$). The expression of Z_s involves quadratics and exponentials, and its global shape is illustrated in Fig. 4, where it is plotted as a function of Δ_0 and n_0. The main characteristic of the Z_s diagram is the presence of a fold in the parameter space. For $\Delta_0 = -1.2$, the fold is relatively smooth, at $n_0 \simeq 3 \times 10^8$. As Δ_0 decreases, the fold shifts towards higher n_0 values and becomes stiffer. Linear stability analysis of the solutions shows that the stationary solution is unique and stable on the fold, for our experimental conditions. For $-1.6 < \Delta_0 < -1.2$, the system presents an eigenfrequency in the vicinity of the fold and the damping rate decreases. This allows for relaxation oscillations to show up. Finally, for $\Delta_0 < -1.6$ and $n_0 \simeq 3.5 \times 10^8$, a bifurcation towards bistability occurs. The properties described above are invariant under small changes of the other parameters.

As the stationary solutions are always stable for the parameters corresponding to experimental conditions, there are no deterministic instabilities. However, because of the existence of an eigenfrequency in the vicinity of the fold, relaxation oscillations driven by noise can appear. To evaluate this effect, white noise with amplitude ζ is added to Eqs. (6) on I_+ or n_0 by replacing the parameter I_+ (n_0) by $(1 + \zeta)I_+$ [$(1 + \zeta)n_0$]. Both cases give similar results.

Time evolution and the spectral analysis obtained from this stochastic model well reproduce the main features of the experimental observations. In particular, we find that N and Z evolve at different time scales, as illustrated in Fig. 5. The maximum of the spectrum envelope of Z corresponds to the presence of an eigenfrequency in the system. As observed in experiments (Fig. 2), no component at frequencies above 5 Hz appears in the N spectrum. The fold increases the sensitivity of the system to noise, as illustrated in Fig. 6a. The maximum around $\Delta_0 \approx -1.5$ evidences an enhancement of the sensitivity by 1 order of magnitude. This allows the system to be driven by the noise, thus displaying relaxation oscillations.

Although the noisy dynamics prevents us from direct observation of curves like those in Fig. 4, the presence of a fold in the phase space has an observable consequence on the probability distribution of N and Z. Indeed, as the slope of the curves in Fig. 4 is higher on the fold than on its sides, the residence time of the system should present a minimum on the fold, and therefore, the probability distributions of N and Z exhibit a minimum on the fold. This prediction is confirmed by the experimental observations, as it can be deduced easily from Fig. 3.

The behavior discussed here is typical of systems presenting internal stochastic resonance. Stochastic resonance (SR) generates coherent motion—e.g., a periodic motion—when noise is added to a system [11]. In particular, SR implies a nonmonotonic dependence of the signal to noise ratio (SNR) in the response of the system as a function of the noise amplitude. In stable autonomous

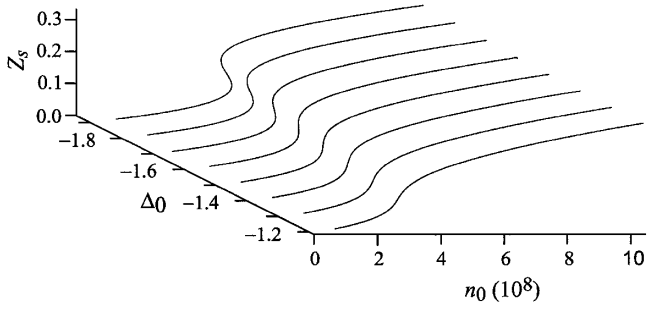

FIG. 4. Stationary solutions of Eqs. (6) versus n_0 and Δ_0. The figure represents Z_s. Bistability occurs for $\Delta_0 < -1.6$. Other parameters are $I_+ = 3$, $\omega_B' = 4.9 \times 10^9\ \mathrm{s^{-1}\,m^{-1}}$, $z_0 = 0.06$ m, $S = 3 \times 10^{-6}\ \mathrm{m^2}$, and $B = 3\ \mathrm{s^{-1}}$.

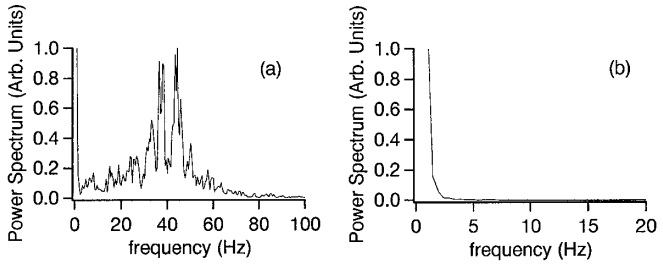

FIG. 5. Power spectra obtained by resolving Eqs. (6) with parameters of Fig. 4 and $n_0 = 3.28 \times 10^8$ and $\Delta_0 = -1.5$. White noise is applied to I_+ with $\zeta = 2 \times 10^{-5}$. In (a), Z and in (b), N. The scales are linear. Integration is performed on 10 s, for comparison with experimental data. The multiple peak structure vanishes when much larger integration times are used.

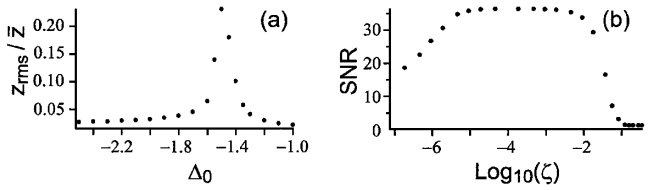

FIG. 6. In (a), theoretical noise amplitude (the ratio of the rms and average values of z) versus Δ_0. In (b), plot of the SNR (ratio of the peak height by the noise level) as a function of the relative noise level. Parameters are the same as in Fig. 4 except that in (a), $n_0 = 3.2 \times 10^8$ and white noise is applied on n_0 with $\zeta = 2 \times 10^{-2}$, and in (b), $n_0 = 3.28 \times 10^8$, $\Delta_0 = -1.5$, and white noise is applied on I_+.

systems close to a supercritical Hopf bifurcation, one observes a behavior usually referred to as *internal SR* or *coherence resonance*, with the same properties as SR [12–14]. In our system, in the vicinity of the fold, we are in a similar situation, as the stable point is a focus with a vanishing damping rate. In Fig. 6b, we have plotted the SNR of the frequency peak of Fig. 5 versus ζ. The nonmonotonic behavior clearly appears. However, it presents a plateau rather than a well defined peak, as usually found in the literature [11]. Thus in the present model, the instabilities are related to the existence of an internal SR behavior of the system. This could have several interesting consequences on the dynamics of the cloud, in particular if the spatial distribution of the atoms is taken into account: for example, stochastic resonance is known to often lead to global synchronization of spatially extended systems.

In conclusion, we have characterized the dynamics of the instabilities experimentally observed in a cold atomic cloud. A simple model allows us to reproduce the essential features of the experimental signals and to identify the shadow effect as responsible for the nonlinearity associated with the instabilities. The dynamics is interpreted as noise-driven relaxation oscillations of the system, through a stochastic resonancelike phenomenon. This is, to our knowledge, the first evidence of such a phenomenon in a "simple" atomic system. Let us recall that our results concern the experimental configuration with counterpropagating beams resulting from the reflection of the forward beams. In a configuration with six independent beams, instabilities are also observed. In a future study, it should be interesting to check if the same physical mechanisms are able to explain them. Indeed, in such a configuration, the shadow effect does not disappear, although it no longer displaces the c.m. location. Moreover, at larger cloud populations, the above model displays a richer dynamics, presenting bistability and periodic instabilities, which could enhance the stochastic resonance. We postpone their detailed analysis to a forthcoming work.

The authors gladly acknowledge P. Glorieux, G. Grynberg, P. Szriftgiser, P. Verkerk, and V. Zehnlé for fruitful discussions. The Laboratoire de Physique des Lasers, Atomes et Molécules is "Unité Mixte de Recherche de l'Université de Lille 1 et du CNRS" (UMR 8523). The Centre d'Etudes et de Recherches Lasers et Applications (CERLA) is supported by the Ministère chargé de la Recherche, the Région Nord-Pas de Calais and the Fonds Européen de Développement Economique des Régions.

*Present address: Institut Non linéaire de Nice, Université de Sophia-Antipolis, F-06560 Valbonne, France.

[1] S. Chu, Rev. Mod. Phys. **70**, 685 (1998); C. Cohen-Tannoudji, Rev. Mod. Phys. **70**, 707 (1998); W. Phillips, Rev. Mod. Phys. **70**, 721 (1998).
[2] T. Walker, D. Sesko, and C. Wieman, Phys. Rev. Lett. **64**, 408 (1990); D. W. Sesko, T. G. Walker, and C. E. Wieman, J. Opt. Soc. Am. B **8**, 946 (1991).
[3] I. Guedes, M. T. de Araujo, D. M. B. P. Milori, G. I. Surdutovich, V. S. Bagnato, and S. C. Zilio, J. Opt. Soc. Am. **11**, 1935 (1994); V. S. Bagnato, L. G. Marcassa, M. Oria, G. I. Surdutovich, R. Vitlina, and S. Zilio, Phys. Rev. A **48**, 3771 (1993).
[4] In fact, the measured center of mass is weighted by the fluorescence rate of the atoms.
[5] D. Wilkowski, These de l'Université des Sciences et Techniques de Lille, 1997 (unpublished).
[6] J. Dalibard, Opt. Commun. **68**, 203 (1988).
[7] Multiple scattering can *indirectly* affect the c.m. motion, because it modifies the density of the cloud, thus its optical thickness and the shadow effect.
[8] D. Wilkowski, J. C. Garreau, and D. Hennequin, Eur. Phys. J. D **2**, 157 (1998).
[9] L. Marcassa, V. Bagnato, Y. Wang, C. Tsao, J. Weiner, O. Dulieu, Y. B. Band, and P. S. Julienne, Phys. Rev. A **47**, R4563 (1993).
[10] C. G. Townsend, N. H. Edwards, C. J. Cooper, K. P. Zetie, C. J. Foot, A. M. Steane, P. Szriftgiser, H. Perrin and J. Dalibard, Phys. Rev. A **52**, 1423 (1995).
[11] L. Gammaitoni, P. Hänggi, P. Jung, and F. Marchesoni, Rev. Mod. Phys. **70**, 223 (1998).
[12] Lin I and Jeng-Mei Liu, Phys. Rev. Lett. **74**, 3161 (1995).
[13] A. S. Pikovsky and J. Kurths, Phys. Rev. Lett. **78**, 775 (1997).
[14] A. Neiman, P. I. Saparin, and L. Stone, Phys. Rev. E **56**, 270 (1997).